Struct Multidisc Optim (2006)
DOI 10.1007/s00158-005-0530-4

RESEARCH PAPER

Z.-D. Ma · H. Wang · N. Kikuchi · C. Pierre · B. Raju

Experimental validation and prototyping of optimum designs obtained from topology optimization

Received: 21 October 2004 / Revised manuscript received: 7 February 2005 / Published online: 19 January 2006

Abstract This paper provides, through both numerical analyses and physical tests, a validation of the optimality of structural designs obtained from a topology optimization process. Issues related to the manufacturability of the topology-optimized design are first addressed in order to develop structural specimens suitable for experimental validation. Multidomain and multistep topology optimization techniques are introduced that, by embedding the designer's intuition and experience into the design process, allow for the simplification of the design layout and thus for a better manufacturability of the design. A boundary identification method is also proposed that is applied to produce a smooth boundary for the design. An STL (STereo Lithography) file is then generated and used as input to a rapid prototyping machine, and physical specimens are fabricated for the experiments. Finally, the experimental measurements are compared with the theoretical and numerical predictions. Results agree extremely well for the example problems considered, and thus the optimum designs pass both virtual and physical tests. It is also shown that the optimum design obtained from topology optimization can be independent of the material used and the dimensions assumed for the structural design problem. This important feature extends the applicability of a single optimum design to a range of different designs of various sizes, and it simplifies the prototyping and experimental validation since small, inexpensive prototypes can be utilized. This could result in significant cost savings when carrying out proof-of-concept in the product development process.

Z.-D. Ma (✉) · N. Kikuchi · C. Pierre
Department of Mechanical Engineering, University of Michigan, 2250 G. G. Brown Bldg., Ann Arbor, MI 48109-2125, USA
E-mail: {mazd, kikuchi, pierre}@umich.edu

H. Wang
MKP Structural Design Associates, Inc., 3003 Washtenaw Ave., Ann Arbor, MI 48104-5107, USA
E-mail: wanghui@mkpsd.com

B. Raju
U.S. Army Tank-Automotive and Armaments Command

Keywords Topology optimization · Experimental validation · Optimal design · Structural dynamics · Noise and vibration

Introduction

Topology optimization has received extensive attention since the groundbreaking paper of Bendsøe and Kikuchi (1988). To date significant progress has been made using a variety of approaches, as evidenced by the number of commercial codes that have been developed and the variety of applications that have been treated (see Rozvany et al. 1994; Bendsøe 1995, 2003; Hassani and Hinton 1999). However, despite the great promise held by topology optimization, there is still a gap between the theory and real engineering design applications. Specifically, laying out an optimum design with the effectiveness and efficiency required of an engineering product remains a considerable challenge. In an effort to fill this gap, we address in this paper some fundamental issues related to the manufacturability and proof-of-concept of new structural designs generated by topology optimization.

A critical issue in the applicability of topology optimization to a practical engineering design problem is the manufacturability of the design. The optimum design obtained from a standard topology optimization process tends to be too complicated and without a smooth boundary; it is therefore quite difficult to manufacture. Ambrosio and Buttazzo (1993) first introduced a scheme to simplify the structural shape using a perimeter control, which was further implemented by Haber et al. (1996) with a finite element method. This technique allows the designer to control the number of holes in the optimal design and to establish their characteristic length scale. Sigmund and Petersson (1998) provided a survey of procedures dealing with issues such as checkerboards, mesh dependencies, and local minima occurring in the topology optimization processes. The checkerboard problem refers to the formation of regions of alternating solid and void elements ordered in a checkerboardlike fashion. The mesh-dependence problem refers to obtaining

qualitatively different solutions for different mesh sizes or discretizations. Local minima refers to the problem of obtaining different solutions to the same discretized problem when choosing different algorithmic parameters. Petersson and Sigmund (1998) further proposed a slope-constrained topology optimization method in which the design set is restricted by enforcing pointwise bounds on the density slope. Using this method, the checkerboard patterns and other numerical anomalies can be minimized. Belytschko et al. (2003) and Guest et al. (2004) studied topology optimization methods with projection functions and regularizations and with the use of nodal design variables to achieve the minimum length scale. Xu and Ananthasuresh (2003) developed a freeform skeletal shape optimization method using Bezier curves after conducting a topology optimization process for the compliant mechanism design. Wang et al. (2004) introduced the so-called nonlinear diffusion methods to the regularization of topology optimization problems, which have a close relationship with the diffusion methods used in the fields of materials and digital image processing. It was shown that a nonlinear or anisotropic diffusion process not only leads to a suitable problem regularization but also exhibits strong "edge"-preserving characteristics. While the aforementioned methods have been effectively developed, in this paper we introduce a multidomain, multistep topology optimization process (MMTO), which can be combined with these existing methods to further improve the manufacturability of the final design.

The multidomain topology optimization technique (MDTO) enables the effective design of a complex engineering structure by allowing the designer to control the material distribution among subdomains during the optimal design process and to follow a desired pattern or tendency for the material distribution. The multistep topology optimization technique (MSTO) allows the designer to lay out a design from a coarser mesh and then refine it repeatedly until the desired finer design is obtained. Also, various filters can be applied in between the refinements, for example, to remove unwanted structural details or submembers and thus further improve the manufacturability of the final design. Other filters may include those to adjust the material distribution in a desired way, to smooth the structural boundaries, to control the member size, etc. These filters can be realized through a computational algorithm or by hand through a well-developed graphic user interface. A major feature of the combined MDTO and MSTO approach (MMTO) is that the designer has more control over the structural forming process such that intuition and experience can be effectively utilized.

Another issue affecting fabrication is that the design layout produced by the topology optimization process usually features nonsmooth, steplike boundaries. Here we propose to utilize a simple scheme to achieve piecewise smooth boundaries for the structure. These identified structural boundaries can then be used to generate a finite element model for virtual prototyping or an STL file for physical fabrication. For example, in this study, prototypes were fabricated with a rapid prototyping machine using the STL output directly obtained from the topology optimization process. It is also shown in this paper that reduced-size ABS (acrylonitrile butadiene styrene) plastic prototypes can be used for proof-of-concept because the optimum design (including topology, shape, and size) obtained from the design process is independent of the material used and the size of the actual structure, provided a proper scaling factor is applied. The influences of dimension and material type are discussed in order to relate the simplified prototypes to the full-size structure. The ultimate goal of this research is to develop a systematic verification tool that can be used to assess the optimality of a structural design in a general, efficient, and cost-effective manner. The aforementioned important feature of material and size independence of the design is proven in the general case through a theoretical analysis. This important result extends the applicability of the optimum design and simplifies the prototyping and test process, thus alleviating the need for building full-size prototypes and performing expensive tests at the proof-of-concept stage.

The remainder of this paper is organized as follows. The multidomain topology optimization (MDTO) and multistep topology optimization (MSTO) methods are described first. Then, the fabrication process of truly optimum structures is introduced, including the postprocessing of the optimization results and the rapid prototyping. This is followed by a description of experimental investigation for the prototypes, including the validation of the test results using numerical simulations. Finally, the influences of dimension and material type on the optimum design are discussed.

Multidomain topology optimization

In the standard topology optimization method, a structure is optimized within a single structural domain, subject to a given amount of material for the entire structure, and the material is automatically distributed throughout the structure without any interaction with the designer. This process, however, leaves little flexibility to the designer for controlling the material distribution in a way he/she may desire. For example, a designer may want to distribute more material in a certain subdomain of the structure and less material in another. To address this issue, a multidomain topology optimization (MDTO) technique has been developed in Ma et al. (2002) based on a generalized sequential approxi-

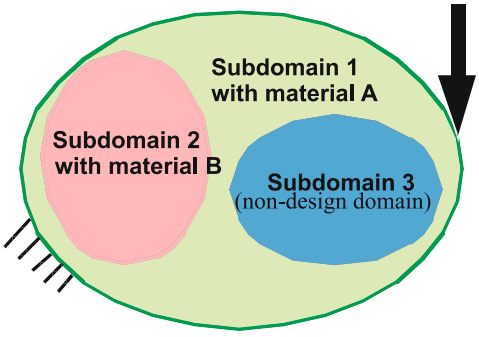

Fig. 1 A multidomain topology optimization problem

mate optimization (GSAO) algorithm introduced by Ma and Kikuchi (1995).

In contrast to single domain topology optimization, in which a given amount of the material is assigned to the entire design domain, MDTO allows the designer to assign different amounts of the material, or even different materials, to the different subdomains of the structure. For example, Fig. 1 shows a structural domain divided into several subdomains, where a certain amount of material A is distributed into subdomain 1, and a different amount of material B is distributed into subdomain 2. Furthermore, subdomain 3 is considered as a nondesign domain, where the material distribution is not allowed to change at the current design stage.

In the general case, the MDTO problem can be formulated as

$$\begin{aligned} &\text{Minimize} \quad f(\mathbf{X}) , \\ &\text{Subject to: } h_j(\mathbf{X}) \le 0 \ (j = 1, 2, \ldots, m) , \\ &\qquad \underline{x}_i \le x_i \le \overline{x}_i \ (i = 1, 2, \ldots, n) \\ &\qquad (\text{and state equations}) , \end{aligned} \tag{1}$$

where $f = f(\mathbf{X})$ denotes the objective function; $h_j = h_j(\mathbf{X})$ denotes the jth constraint function for the volume (or weight) of the jth substructure in the jth subdomain (where $j = 1, 2, \ldots, m$); m is the total number of the subdomains; $\mathbf{X} = \{x_1, x_2, \ldots, x_n\}^{\mathrm{T}}$ denotes the vector of the design variables, where n is the total number of design variables; and $\underline{x}_i$ and $\overline{x}_i$ are the lower and upper bounds of design variable x_i, respectively. Note that $f(\mathbf{X})$ in (1) also needs to satisfy the state equations for the structural problem at hand.

The optimization problem, (1), usually involves a very large number of design variables, and thus it requires a highly efficient optimization algorithm. Because traditional mathematical programming methods are not practical for dealing with so many design variables, optimality criteria (OC) methods (e.g., those used in Bendsøe and Kikuchi 1988 and Ma et al. 1995) and sequential approximate optimization (SAO) methods, such as SLP (sequential linear programming), SQP (sequential quadratic programming), CONLIN (convex linearization; Fleury and Braibant 1986), and MMA (method of moving asymptotes; Svanberg 1987) were employed for solving the problem. Ma and Kikuchi (1995) developed a generalized SAO (GSAO) method that can be considered an enhancement and generalization of the previous OC and SAO algorithms and that includes the aforementioned algorithms as special cases. A selected GSAO algorithm is introduced in this paper that can be considered an extension of the CONLIN and OC algorithms. More details regarding the other GSAO algorithms can be found in Ma and Kikuchi (1995).

Using the SAO approach, the original optimization problem (1) can be transformed into a series of approximate optimization problems (AOP). By properly choosing the parameters in the GSAO method, the AOP can always be made convex and therefore be solved by using a dual method. The dual problem of an AOP can be written as

$$\begin{aligned} &\underset{\boldsymbol{\lambda}}{\text{maximize}} \ L^k(\mathbf{X}^*(\boldsymbol{\lambda}), \boldsymbol{\lambda}) \\ &\text{subject to } \lambda_j > 0 \ (j = 1, 2, \ldots, m) , \end{aligned} \tag{2}$$

where $\boldsymbol{\lambda} = \{\lambda_1, \lambda_2, \ldots, \lambda_m\}^{\mathrm{T}}$ denotes the vector of the dual variables, and one has

$$\begin{aligned} L^k(\mathbf{X}^*(\boldsymbol{\lambda}), \boldsymbol{\lambda}) &= f_0^k + \sum_{j=1}^{m} \lambda_j h_{0j}^k \\ &+ \sum_{i=1}^{n} \left[a_i^k \left(x_i^*\right)^{\xi_i} + \sum_{j=1}^{m} \lambda_j b_{ji}^k \left(x_i^*\right)^{\zeta_i} \right] , \end{aligned} \tag{3}$$

where

$$\begin{aligned} a_i^k &= \frac{1}{\xi_i} \left(x_i^k\right)^{1-\xi_i} f_{,x_i}^k , \\ b_{ji}^k &= \frac{1}{\zeta_i} \left(x_i^k\right)^{1-\zeta_i} h_{j,x_i}^k , \\ f_0^k &= f(\mathbf{X}^k) - \sum_{i=1}^{n} a_i^k \left(x_i^k\right)^{\xi_i} = f(\mathbf{X}^k) - \sum_{i=1}^{n} \frac{1}{\xi_i} f_{,x_i}^k x_i^k , \\ h_{0j}^k &= h_j\left(\mathbf{X}^k\right) - \sum_{i=1}^{n} b_{ji}^k \left(x_i^k\right)^{\zeta_i} = h_j(\mathbf{X}^k) - \sum_{i=1}^{n} \frac{1}{\zeta_i} h_{j,x_i}^k x_i^k , \end{aligned} \tag{4}$$

where $x_i^k (i = 1, 2, \ldots, n; k = 1, 2, \ldots)$ are the design variables obtained at the previous, or $(k-1)$th, iteration (for $k = 1$, $x_i^1 (i = 1, 2, \ldots, n)$ are the initial design variables), and

$$f_{,x_i}^k = \left.\frac{\partial f}{\partial x_i}\right|_{\mathbf{X}=\mathbf{X}^k} \text{ and } h_{j,x_i}^k = \left.\frac{\partial h_j}{\partial x_i}\right|_{\mathbf{X}=\mathbf{X}^k} .$$

ξ_i and ζ_i in (3) and (4) are determined by the parameters ξ_i^+ and ξ_i^- and by the sign of the derivatives of the objective function and constraint functions, namely

$$\xi_i = \begin{cases} \xi_i^+ \text{ if } f_{,x_i}^k > 0 \\ \xi_i^- \text{ if } f_{,x_i}^k < 0 \end{cases} , \quad \zeta_i = \begin{cases} \xi_i^+ \text{ if } h_{j,x_i}^k > 0 \\ \xi_i^- \text{ if } h_{j,x_i}^k < 0 \end{cases} , \tag{5}$$

where ξ_i^+ and ξ_i^- are the parameters introduced by the GSAO method. To simplify the problem, in this paper we can have

$$\xi_i^+ = \xi^+ \text{ and } \xi_i^- = \xi^- \quad (\text{for } i = 1, 2, \ldots, n) , \tag{6}$$

where ξ^+ and ξ^- are two given parameters (the selections of their values will be discussed later). In (2), $\mathbf{X}^*(\boldsymbol{\lambda}) = \{x_1^*(\boldsymbol{\lambda}), x_2^*(\boldsymbol{\lambda}), \ldots, x_n^*(\boldsymbol{\lambda})\}^{\mathrm{T}}$ is a function of the dual variables and can be obtained by using the following suggested GSAO updating rule:

$$x_i^* = \begin{cases} \underline{x}_i^k & \text{if } w_i x_i^k \le \underline{x}_i^k , \\ w_i x_i^k & \text{if } \underline{x}_i^k < w_i x_i^k < \bar{x}_i^k , \\ \bar{x}_i^k & \text{if } w_i x_i^k \ge \bar{x}_i^k , \end{cases} \tag{7}$$

where $\underline{x}_i^k = \max\{(1-\mu)x_i^k, \underline{x}_i\}$ and $\bar{x}_i^k = \min\{(1+\mu)x_i^k, \bar{x}_i\}$ are so-called moving limits, while μ $(0 < \mu < 1)$ is a given parameter, and one has

$$w_i = \begin{cases} \left(-\dfrac{q_i^-}{f_i^+ + q_i^+} \right)^{\eta_i} & \text{if } f_{,x_i}^k > 0 \\ \left(-\dfrac{f_i^- + q_i^-}{q_i^+} \right)^{\eta_i} & \text{if } f_{,x_i}^k < 0 \end{cases}, \tag{8}$$

where

$$q_i^+ = \sum_+ \lambda_j h_{j,x_i}\,,\ q_i^- = \sum_- \lambda_j h_{j,x_i}\,,\ f_i^+ = f_{,x_i}^k \left(f_{,x_i}^k > 0 \right),$$
$$f_i^- = f_{,x_i}^k \left(f_{,x_i}^k < 0 \right),\ \text{and}\ \eta_i = \frac{1}{\xi_i^+ - \xi_i^-}\,, \tag{9}$$

where $\sum_+$ represents the summation over the terms that satisfy $h_{j,x_i}^k > 0$ and $\sum_-$ is the summation over the other terms.

Note that the CONLIN algorithm developed by Fleury and Braibant (1986) is a special case of (8) when $\xi^+ = 1$ and $\xi^- = -1$, and that the OC algorithm (e.g., the one used in Bendsøe and Kikuchi 1988) can be obtained by assuming $m = 1$ and $\xi^+ = 1$ and that $f_{,x_i}^k < 0$ and $h_{j,x_i}^k > 0$ are satisfied for all design variables. In the general case, for the topology optimization problem defined in this paper, we can fix the parameter ξ^+ as $\xi^+ = 1$ and vary the parameter ξ^- between -1 and -9. The power parameter η_i in (8), which is determined by ξ^+ and ξ^- using the last equation in (9), has the same effect on the optimization process as the power parameter used in the traditional OC algorithm (e.g., see Berke and Khot 1987), namely, a large value of η_i increases the convergence speed, but a smaller value of η_i improves the smoothness of the convergence of the optimization process. For some typical problems, other values of ξ^+ and ξ^- can also be used, which can be selected through numerical experiments. Furthermore, different values of ξ^+ and ξ^- can be used for different design variables or determined using secondary derivative information. Discussions related to these advanced uses are, however, omitted from this paper.

Figure 2 illustrates an example engineering application of the MDTO approach to the redesign of a truck chassis frame. In this problem, it is assumed that the rails and the bumper cannot be changed at the design stage; these are shown as the blue areas in Fig. 2. The objective function is a combination of two design goals: (1) minimize the mean in-plane compliance of the frame and (2) maximize the first five eigenfrequencies of the in-plane modes of the frame. Figure 2 depicts the optimum structures obtained from (a) a single-domain topology optimization and (b) a multidomain topology optimization for the same objective function and the same total amount of material used to build the frame. As a first try, a single-domain topology optimization was conducted in which the connectors were allowed to be placed anywhere in the design domain between the two rails (Fig. 2a), with a constraint on the total material density (20%) for the connectors. Figure 2a shows the result from this optimization process. It is seen that the resulting design may not be satisfactory because too much material is assigned to the front part of the frame, which may be difficult to fabricate. Also, this design provides insufficient support in the middle part of the frame for a real vehicle. This undesirable design may be due to the lack of several considerations in the design process, for example, the out-of-plane loads and more accurate boundary conditions and loading conditions. However, it is difficult to account for all such factors in the numerical process because these are dependent on the wide variety of operating conditions of the vehicle.

As a second try, a multidomain topology optimization was conducted in which the material was required to be evenly distributed among the four subdomains (Fig. 2b). As shown in Fig. 2b, the multidomain topology optimization results in a structure that has better (i.e., much more reasonable) material distribution and that can be manufactured more easily. Figure 3 further illustrates the entire design process from initial design to final prototype. A small-scale prototype was actually fabricated using a rapid prototyp-

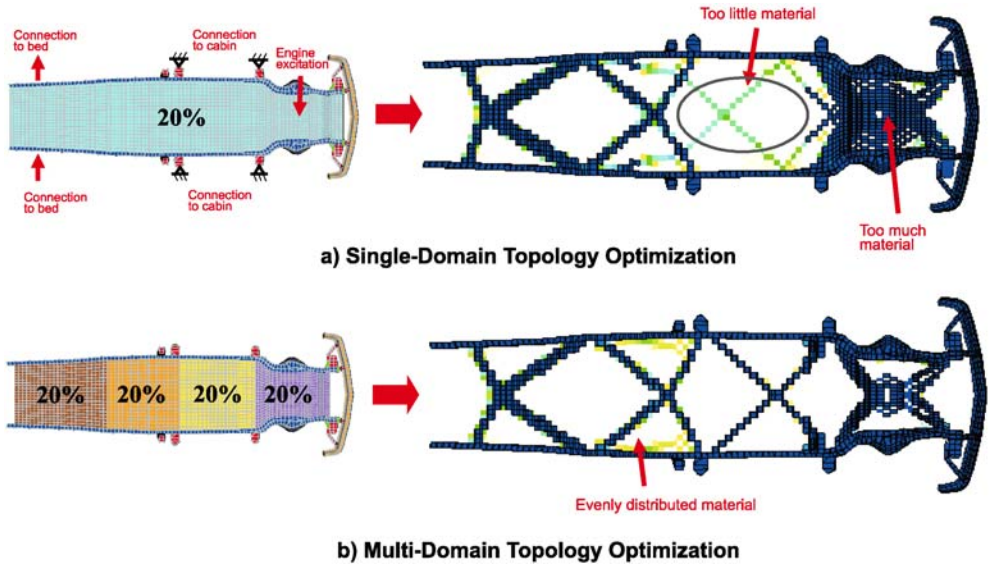

Fig. 2 Comparison of MDTO and SDTO

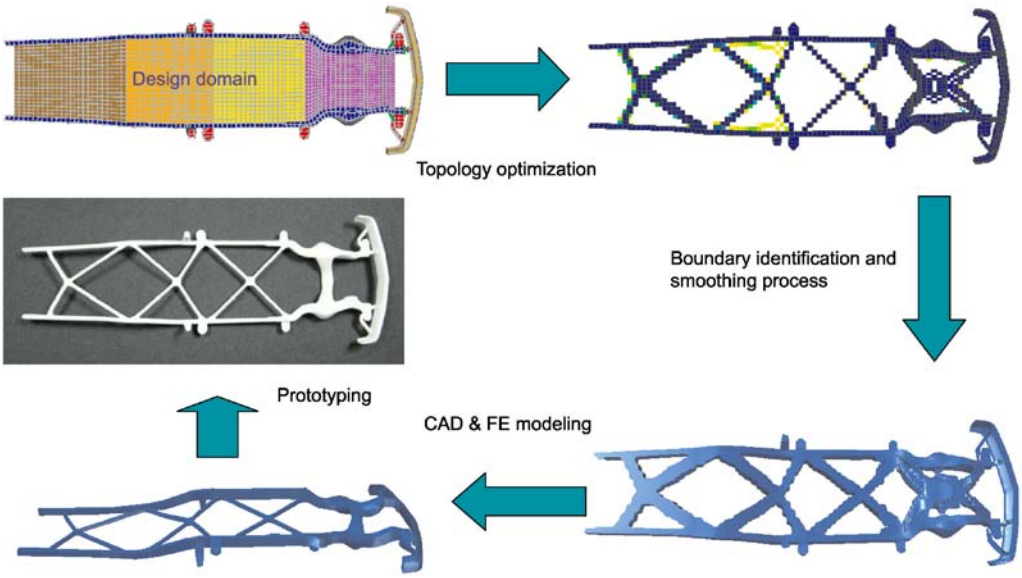

Fig. 3 From initial design to final prototype

ing machine and a composite material (DuraForm GF) of polyamide and glass bead.

Multistep topology optimization

By iterating the optimization process from a rough design to a refined design, the MultiStep Topology Optimization (MSTO) approach can simplify the architecture of the structure and thus significantly improve the manufacturability of the design. Figure 4 illustrates an MSTO process for an example design problem of a (simplified) truck frame. As shown in Fig. 4, the design process begins with defining the design problem (step 1). This is followed by a first topology optimization, which employs a coarse mesh for the purpose of laying out a simple sketch of the structure (step 2). In step 3, the design domain is refined with a finer mesh, and a filtering process is also applied to eliminate the unwanted details from the initial design. Note that various filters can be utilized in this step. The simplest consists of filtering out the material under a given threshold or to fill the material in full when the material density is above a given threshold. Other filters may include those to smooth the structural boundaries, to control the member size, to artificially adjust the material distribution using a numerical rule, etc. These filtering processes can be automated through a computational algorithm, or they can rely on the engineer's intuition along with a well-developed graphic user interface. Detailed dis-

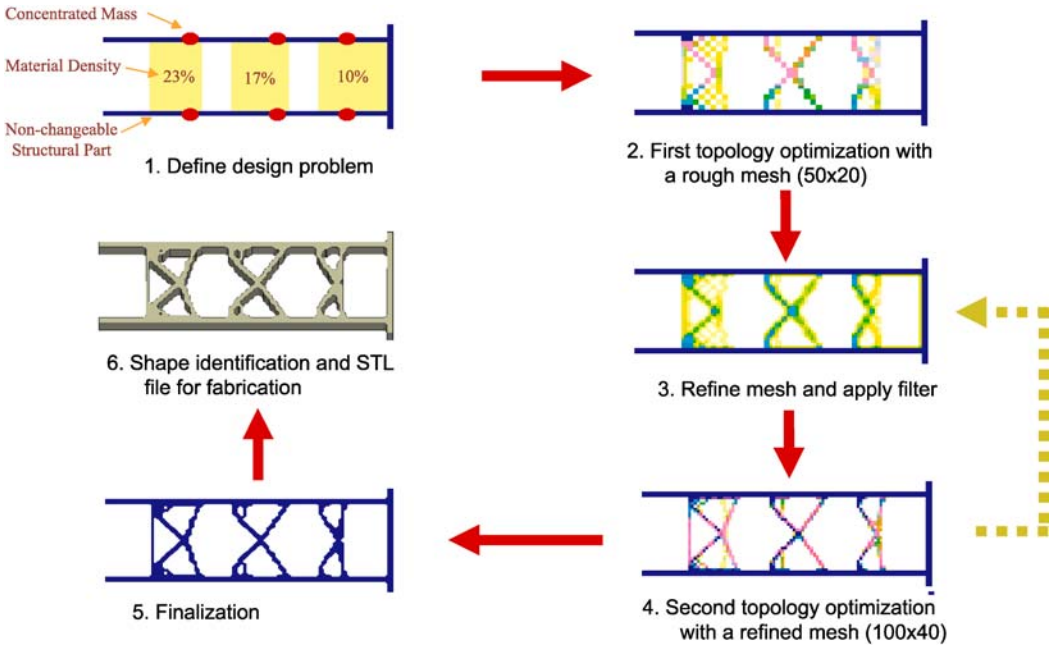

Fig. 4 Multistep topology optimization

cussions regarding these various filter designs are beyond the scope of this paper and warrant a separate publication.

The second topology optimization is then applied to obtain a satisfactory refined outline of the structure (step 4). Note that this step is essential to ensure the optimality after step 3. Steps 3 and 4 may be repeated until a desired result is obtained. Finally, after finalizing the structure (step 5), a shape-identification process is applied and an STL (STereo Lithography) file is generated for the manufacturing process. As can be observed in Fig. 4, this MDTO process results in a simplified geometry for the structure, which can significantly improve manufacturability and reduce fabrication costs. Note that for this example the objective was to maximize the first in-plane bending eigenfrequency of the frame structure subject to the given material density of 40%. More details about this design problem can be found in Ma et al. (2003). Also note that a smoothing algorithm was used in step 5 to identify the geometric shape of the final design. This is described in the next section.

Automatic postprocessing for shape identification

To identify the final shape of the optimal design resulting from topology optimization for manufacturing or further shape optimization, an automatic postprocessor was developed. This postprocessing also provides the capability of automatic finite element mesh generation for virtual prototyping. To identify the final structural geometry, first the material density of each element from the topology optimization is normalized by a filtering algorithm. Then, the material density is calculated at each node using an averaging method such as that used for calculating the nodal stress in a standard finite element postprocessor. In this process, the elements with material are assigned a value of 1 and other elements a value of 0. The nodal densities of the material are therefore in the range [0, 1]. The boundaries between the structural portions with and without material are then identified as contour lines at a value of 0.5. As a result, piecewise smooth boundaries can be identified for the structure. This boundary identification process is illustrated in Fig. 5. First the nodal material densities are calculated (blue). Then the 0.5-value points are determined (red). The piecewise smooth boundaries are then obtained by connecting these middle points. It can be seen that with this algorithm the total amount of material is almost unchanged. More advanced algorithms, such as B-spline fitting, could be employed to further improve the smoothness of the boundaries. Also, manufacturing constraints can be considered based on the fabrication requirements of the actual structure.

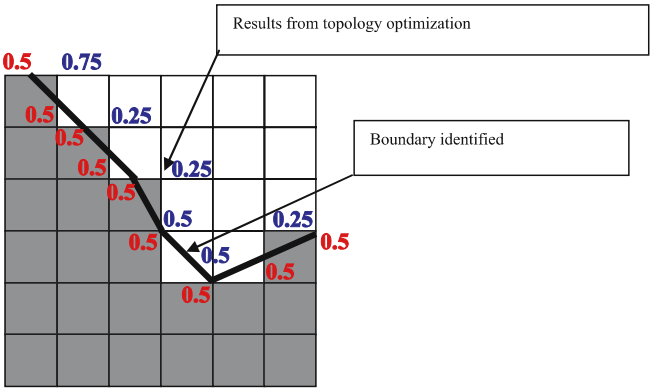

Fig. 5 Boundary identification

Figure 6 illustrates an example design problem considered in this paper, which will be used for experimental validation. As depicted in Fig. 6, a beamlike structure is designed with the design domain colored green and the nondesign domains in blue. The solid material on the left and right sides of the structure represents the fixtures needed for conducting the experiment. The objective of the design problem is to minimize the dynamic response (dynamic compliance; see Ma et al. 1993) under a low-frequency sinusoidal excitation, as shown in Fig. 7a. This objective is equivalent to maximizing the fundamental eigenfrequency of the structure (Ma et al. 1995c). The constraint function for the design problem is the overall material density, which equals 43%. This design problem is first modeled by a 92×20 mesh with a total number of 1953 nodes, 1840 four-node plane stress finite elements, and 5520 design variables (including 1840 angular variables) as an initial design step in

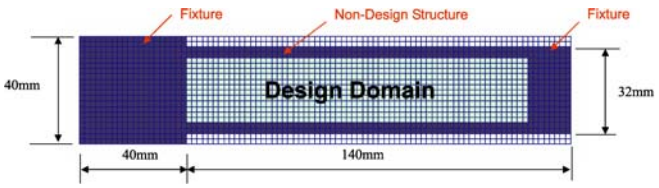

Fig. 6 Defination of design problem

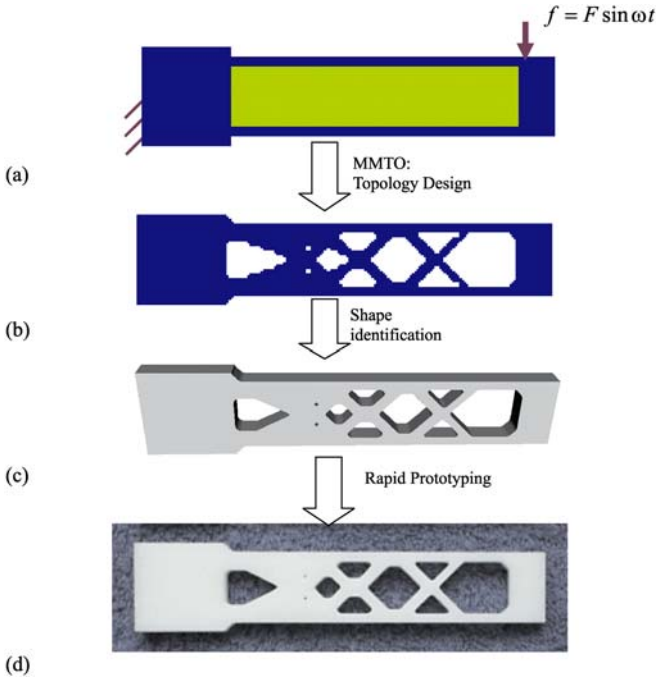

Fig. 7 Post-processing for physical prototyping

the MMTO. This finite element mesh is then refined in the second step to be 184×40, which has a total number of 7585 nodes, 7360 elements, and 22,080 design variables. Figure 7b depicts the optimum structure obtained through this MMTO process. Figure 7c shows the result obtained from the postprocessing tool described in this section, and it demonstrates its effectiveness. The output from this postprocess is an STL file, which is then sent to a rapid prototyping machine for fabrication. Figure 7d shows the physical prototype of the design fabricated from an ABS (acrylonitrile butadiene styrene) material using the rapid prototyping machine. In the next section, the experimental validation of the specimen developed is discussed.

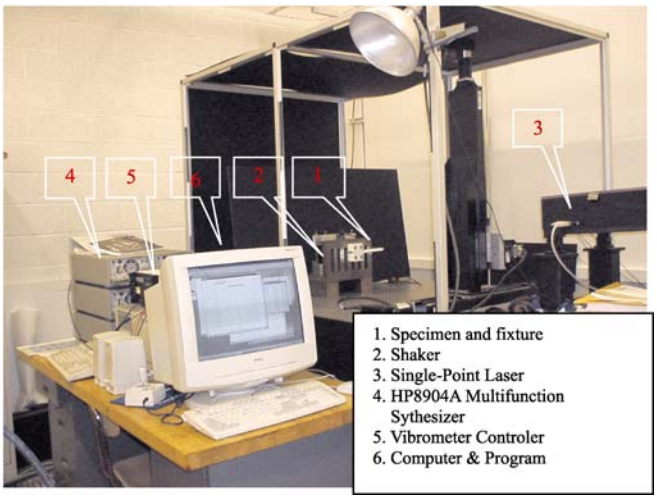

Fig. 8 Experiment setup

Experimental verification

(a) Method and setup

The in-plane natural frequencies of the specimen shown in Fig. 7d were measured using a dynamic testing facility (Fig. 8). The excitation was provided by a shaker (Bruel and Kjaer Type 4809), which was positioned behind the angle plate to which the test specimen was attached. Harmonic signals generated by a Hewlett-Packard 8904A Multifunction Synthesizer were used to drive the shake over a range of frequencies. A single-point laser vibrometry (SPLV) system,

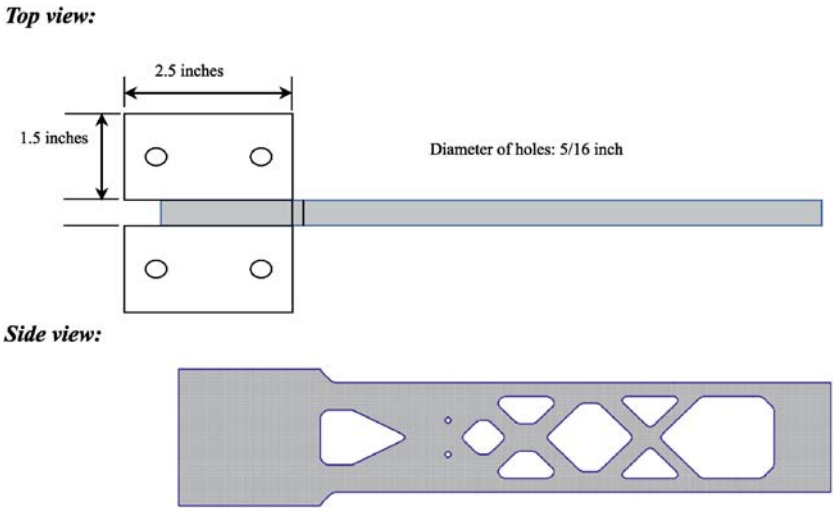

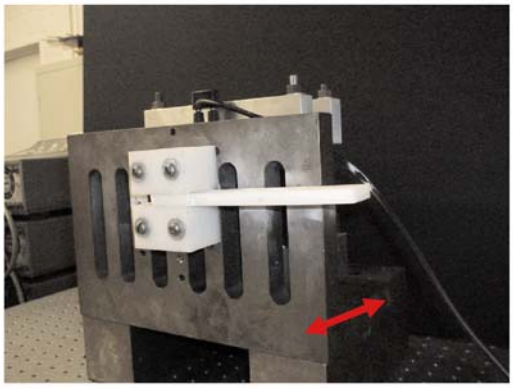

Fig. 9 Physical prototypes

consisting of a Polytec OFV2602 Vibrometer Controller with a Polytec OFV353 Sensor Head, was used to measure the vibration amplitude. The SPLV was mounted on a linear traverse, which allowed it to be moved so as to measure the response at various locations.

A frequency sweep was performed with the SPLV, and the response at the beam tip was measured. At each resonant frequency identified by this sweep, a scan was then performed along the length of the beam by programming the traverse to move in 5-mm increments and measuring the response at each position. Both the vibration amplitude and the phase relative to the excitation were measured.

(b) Specimens

The specimen attached to the fixture is shown in Fig. 9a, where the blocks at the left end provide a sufficient constraint to achieve a fixed boundary condition. Four holes were drilled in the blocks in order to bolt them to the plate in front of the shaker (Fig. 9b). For purposes of comparison, another beam was fabricated, which represented the nominal design and had the same dimensions as the optimum specimen.

(c) Results

The three lowest free vibration natural frequencies of the optimum and the nominal specimens were identified with the frequency sweep process. For the optimum beam they are 322 Hz, 1150 Hz, and 2308 Hz. For the nominal beam one obtains 305 Hz, 1602 Hz, and 3538 Hz. Note that the optimum design, while featuring a 57% weight saving, is still better than the nominal design in terms of the fundamental frequency. The mode shapes obtained for the optimum design are discussed in the next section.

Comparison of virtual prototyping and physical prototyping

In order to compare experimental measurements with numerical results, virtual prototypes of the nominal and optimum designs were developed (Fig. 10). The commercial finite element code MSC/NASTRAN was used in the calculations. The material was again ABS (acrylonitrile butadiene styrene), which has a Young's modulus of 2480 MPa and a specific gravity of 1.05 g/cc. Table 1 shows the excellent agreement between the predicted and the measured values of the three lowest eigenfrequencies. The corresponding mode shapes obtained from the finite element model are shown in Fig. 11, along with the experimental measurements on the top surfaces of the specimens for each frequency. The results in Table 1 also confirm the experimental finding that with a 57% weight saving, the optimum design obtained from the MMTO process has a better performance than the nominal design in terms of the first eigenfrequency.

The deformation shapes of the first three modes predicted from the virtual prototyping are plotted in Fig. 11 with the experimental measurements on the top of the beam.

Table 1 Comparison of numerical results and experimental measurements (Hz)

Mode #	Nominal Design		Optimum Design	
	Numerical	*Experimental*	*Numerical*	*Experimental*
1	283	305	323	322
2	1438	1602	1127	1150
3	3324	3538	2265	2308

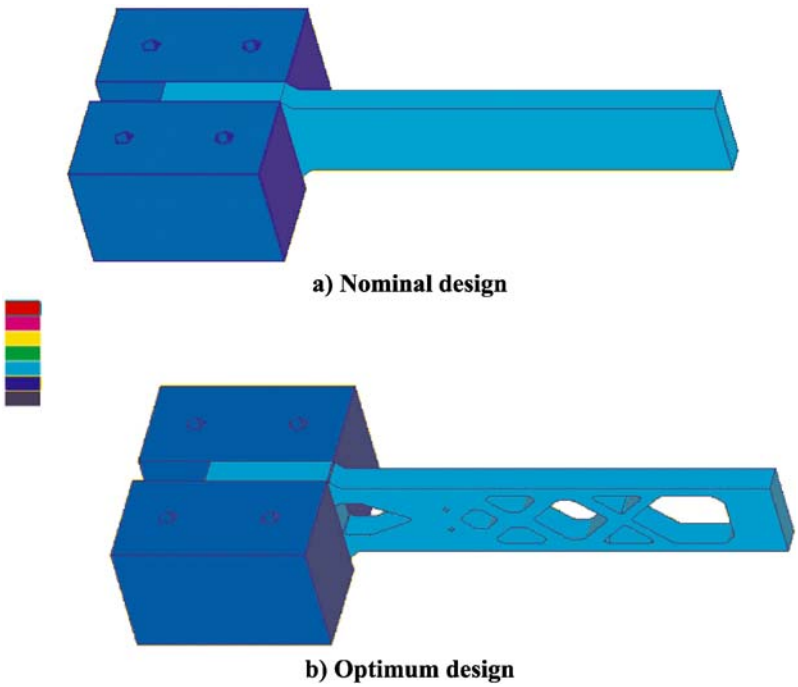

Fig. 10 Virtual prototypes developed for numerical simulation

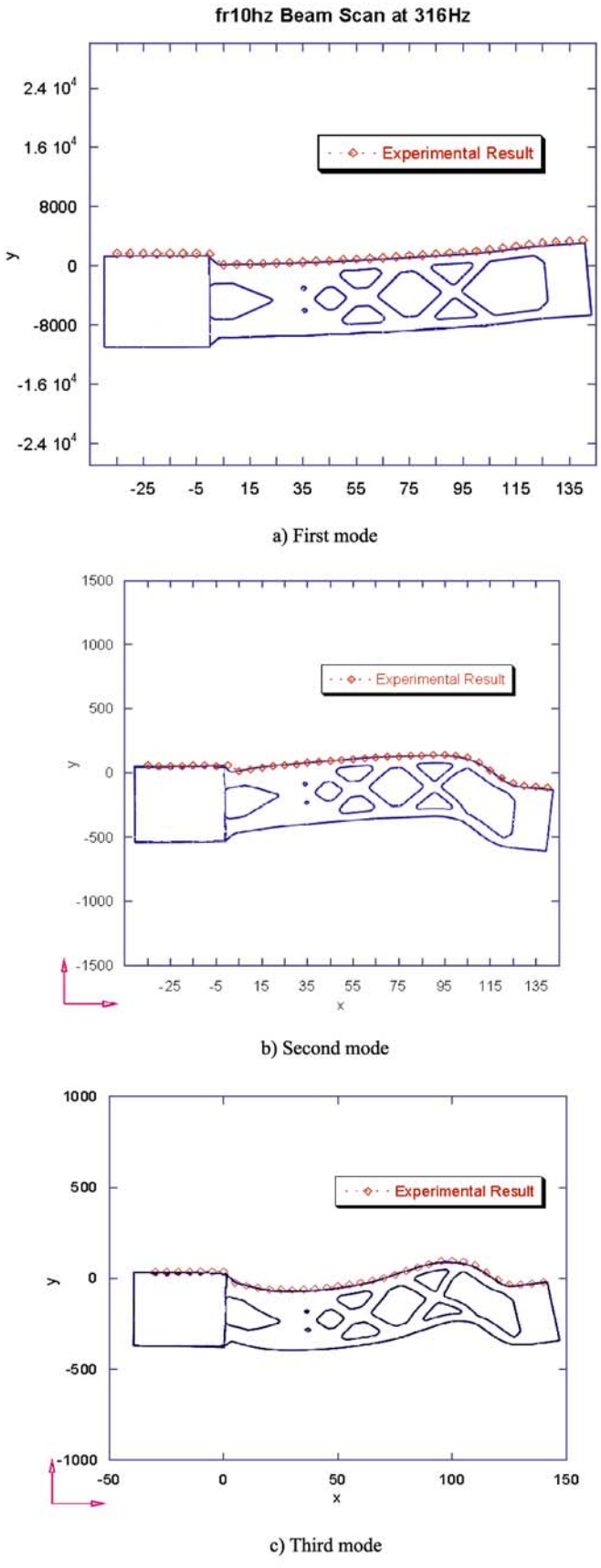

Fig. 11 Comparison of mode shapes for virtual and physical prototypes

It is seen that excellent agreements have also been obtained between the numerical predictions and experimental measurements.

Effects of material property and structural dimensions on the optimum design

The dimensions of the specimen shown in Fig. 7d are $140 \times 40 \times 20$ mm, and it is made of ABS material. It is shown here, however, that the final design shown in Fig. 7c is independent of the material and dimensions assumed. In fact, the performance measure for a different material or a different dimension can be obtained simply by multiplying by a scaling factor. For example, for the eigenfrequencies listed in Table 1, the scaling factor is 3.4 if aluminum is used and 3.3 if steel is used. This is an important feature of the design process as it allows for the application of the same design to structures with different materials and different dimensions.

Even though the state equation in (1) depends on the material and dimensions adopted for the design problem, if the structure is considered to be linear, then the optimal topology (and shape) obtained as the solution of the optimization problem (1) is independent of the material and dimensions used. Thus representative material and dimensions can be used for the design problem. This is proved in what follows for a general structural dynamics problem.

Suppose we obtain the optimal design of a structural system for a certain material (E_0, ρ_0) and dimension (L_0). Using the finite element method, the state equation governing the vibration response can be written as

$$\mathbf{M}_0\ddot{\mathbf{u}}_0 + \mathbf{K}_0\mathbf{u}_0 = \mathbf{f}_0\,, \tag{10}$$

where $\mathbf{u}_0$ and $\mathbf{f}_0$ denote the displacement and force vectors, respectively, and $\mathbf{M}_0$ and $\mathbf{K}_0$ are the mass and stiffness matrices, respectively. For the given material and dimension, we have

$$\mathbf{M}_0 = \int_{\Omega_0} \rho_0 \mathbf{N}^{\mathrm{T}}\mathbf{N}\,\mathrm{d}x_0\,\mathrm{d}y_0\,\mathrm{d}z_0\,, \tag{11}$$

$$\mathbf{K}_0 = \int_{\Omega_0} \mathbf{B}_0^{\mathrm{T}}\mathbf{D}_0\mathbf{B}_0\,\mathrm{d}x_0\,\mathrm{d}y_0\,\mathrm{d}z_0\,, \tag{12}$$

where ρ_0, $\mathbf{N}_0$, $\mathbf{B}_0$, and $\mathbf{D}_0$ are the mass density, shape function, strain matrix, and elasticity matrix, respectively, and Ω_0 is the domain of the structure. Note that for the sake of simplicity, damping is ignored.

Now consider another design problem with a different material and dimensions. By scaling the Young's modulus, mass density, and length variables with those for the previous optimum design, dimensionless variables can be defined as

$$\hat{E} = \frac{E}{E_0}\,, \quad \hat{\rho} = \frac{\rho}{\rho_0}\,, \quad \hat{L} = \frac{L}{L_0}\,, \tag{13}$$

where E, ρ, L are, respectively, Young's modulus, mass density, and characteristic length for the current design. The state equation for the current problem can be written as

$$\mathbf{M}\ddot{\mathbf{u}} + \mathbf{K}\mathbf{u} = \mathbf{f}_0 \,, \tag{14}$$

where, using (13),

$$\mathbf{M} = \int_{\Omega} \rho \mathbf{N}^{\mathrm{T}}\mathbf{N}\,\mathrm{d}x\,\mathrm{d}y\,\mathrm{d}z = \hat{\rho}\hat{L}^3 \int_{\Omega_0} \rho_0 \mathbf{N}^{\mathrm{T}}\mathbf{N}\,\mathrm{d}x_0\,\mathrm{d}y_0\,\mathrm{d}z_0 = \hat{\rho}\hat{L}^3\mathbf{M}_0 \tag{15}$$

$$\mathbf{K} = \int_{\Omega} \mathbf{B}^{\mathrm{T}}\mathbf{D}\mathbf{B}\,\mathrm{d}x\,\mathrm{d}y\,\mathrm{d}z = \hat{E}\hat{L} \int_{\Omega_0} \mathbf{B}_0^{\mathrm{T}}\mathbf{D}_0\mathbf{B}_0\,\mathrm{d}x_0\,\mathrm{d}y_0\,\mathrm{d}z_0 = \hat{E}\hat{L}\mathbf{K}_0 \tag{16}$$

Note that loading and boundary conditions are assumed to be consistent with those in (10).

Substituting (15) and (16) into (14) yields

$$\hat{\rho}\hat{L}^3\mathbf{M}_0\ddot{\mathbf{u}} + \hat{E}\hat{L}\mathbf{K}_0\mathbf{u} = \mathbf{f}_0 \,. \tag{17}$$

Comparing (17) with (10), it is seen that a performance measure for the current system (17) can be obtained from the performance measure for the previous system (10) simply by multiplying by a scaling factor. For example, if natural frequency is the objective function in the optimization problem (10), the scaling factor is

$$\kappa = \sqrt{\frac{E\rho_0 L_0^2}{E_0\rho L^2}} \,. \tag{18}$$

Since multiplying the objective function or constraint functions in (10) by a scalar factor will not affect the solution of the optimization problem, the optimal topology and shape obtained from the design process is independent of the material and dimensions used. Note that the loading and boundary conditions must be consistent for the design problems and that the dimensions must be scaled with the same ratio in all directions. Also note that Poisson's ratio ν may affect the above conclusion. However, materials usually have very close values of ν, so the influence of Poisson's ratio can be ignored in the general case.

Note that in the general case, the scaling factor will be different depending on the objective function defined in the optimization problem. For the strain energy (SE) and mutual strain energy (MSE) of a linear system, the scaling factor is simply

$$\kappa = \frac{EL}{E_0 L_0} \,. \tag{19}$$

Furthermore, if $f = -\mathrm{MSE}/\mathrm{SE}$ is used as the objective function for a compliant mechanism optimization problem, the scaling factor becomes $\kappa = 1$.

Also, note that for a nonlinear problem, the influence of material properties and dimensions may become problem dependent. It is expected, though, that in many cases the above conclusion will still hold, but further investigation on this issue is needed.

Conclusions

This research concerns the processes of optimal design and analysis for a 2D structure. The theoretical foundation of the work is the topology optimization method. Algorithms and programs were developed to transfer the output from topology optimization to CAD files in the STL format. Specimens were manufactured using a rapid prototyping machine, and their free vibration natural frequencies and individual mode shapes were measured. An automatic meshing scheme was developed to produce finite element models of the virtual prototypes, and MSC/NASTRAN was used to determine the natural frequencies and modes shapes. The numerical results agreed with the experimental measurements very well.

The optimality of the designs obtained from topology optimization was verified through experimental and numerical investigations. The efficiency of the proposed design-and-analysis process was demonstrated, suggesting that in the future virtual prototyping can replace part of the experimental investigation.

It was also shown that for a linear elastic problem, the topology of the optimal design is independent of the material properties and geometric dimensions. Once a design is obtained for a given material and dimensions, a simple scaling factor can be applied to recover a design with different dimensions and/or a different material. This is an important feature since a single design may be used for many different applications and a full-scale design may be replaced with a small-scale prototype design, thus reducing significantly design and validation costs.

Acknowledgement This work is supported by the U.S. Army Tank-Automotive and Armaments Command (TACOM). The authors also acknowledge the expert help of Dr. John Judge in the experimental work.

References

Ambrosio L, Buttazzo G (1993) An optimal design problem with perimeter penalization. Calculus Variat Partial Differential Equations 1:55–69

Belytschko T, Xiao SP, Parimi C (2003) Topology optimization with implicit functions and regularization. Int J Numer Methods Eng 57:1177–1196

Bendsøe MP (1995) Optimization of structural topology, shape, and material. Springer, Berlin Heidelberg New York

Bendsøe MP (2003) Topology optimization: theory, methods and applications. Springer, Berlin Heidelberg New York

Bendsøe MP, Kikuchi N (1988) Generating optimal topologies in structural design using a homogenization method. Comput Methods Appl Mech Energ 71:197–24

Berke L, Khot NS (1987) Structural optimization using optimality criteria. In: Soares CAM (ed) Computer aided optimal design: structural and mechanical systems. Springer, Berlin Heidelberg New York, pp 271–311

Fleury C, Braibant V (1986) Structural optimization: a new dual method using mixed variables. Int J Numer Methods Eng 23:409–428

Guest JK, Prevost JH, Belytschko T (2004) Achieving minimum length scale in topology optimization using nodal design variables and projection functions. Int J Numer Methods Eng 61:238–254

Haber RB, Jog CS, Bendsøe MP (1996) A new approach to variable-topology shape design using a constraint on perimeter. Struct Optim 11:1–12

Hassani B, Hinton E (1999) Homogenization and structural topology optimization: theory, practice, and software. Springer, Berlin Heidelberg New York

Ma Z-D, Kikuchi N (1995a) A new method of the sequential approximate optimization. Eng Optim 25:231–253

Ma Z-D, Kikuchi N, Cheng H-C (1995b) Topological design for vibrating structures. Comput Methods Appl Mech Eng 121:259–280

Ma Z-D, Kikuchi N, Cheng H-C, Hagiwara I (1995c) Topological optimization technique for free vibration problems. ASME J Appl Mech 62:200–207

Ma Z-D, Kikuchi N, Hagiwara I (1993) Structural topology and shape optimization for a frequency response problem. Comput Mech 13(3):157–174

Ma Z-D, Kikuchi N, Pierre C, Raju B (2002) Multi-domain topology optimization for vehicle substructure design. In: Proceedings of the 2002 ASME International mechanical engineering congress and exposition, November 2002, New Orleans, LA (IMECE2002-32908), pp 1–10

Ma Z-D, Wang H, Kikuchi N, Pierre C, Raju B (2003) Substructure design using a multi-domain multi-step topology optimization. SAE J Passenger Cars Mech Syst September 2004, pp 1349–1358. Also available as SAE Paper 03B-125

Peterson J, Sigmund O (1998) Slope constraint topology optimization. Int J Numer Methods Eng 41:1417–1434

Rozvany GIN, Zhou M, Sigmund O (1994) Topology optimization in structural design. In: Adeli H (ed) Advances in design optimization. Chapman and Hall, London, pp 340–399

Sigmund O, Petersson J (1998) Numerical instabilities in topology optimization: a survey on procedures dealing with checkerboards, mesh-dependencies and local minima. Struct Optim 16:68–75

Svanberg K (1987) The method of moving asymptotes—a new method for structural optimization. Int J Numer Methods Eng 24:359–373

Wang MY, Zhou S, Ding H (2004) Nonlinear diffusions in topology optimization. Struct Multidisc Optim. DOI 10.1007/s00158-004-0436-6

Xu D, Ananthasuresh GK (2003) Freeform skeletal shape optimization of compliant mechanisms. ASME J Mech Des 125(2):253–261